

Hsa_circ_0014784-induced YAP1 promoted the progression of pancreatic cancer by sponging miR-214-3p

Bingyan Liu^{a,b}, Yongjun Gong^c, Qiyi Jiang^b, Shaoqiu Wu^b, Bo Han^d, Feier Chen^e, Qunjun Lin^f, Ping Wang^g, and Dengke Yang^h

^aTongji University School of Medicine, Shanghai, China; ^bDepartment of Interventional Radiology, Tongren Hospital, Shanghai Jiaotong University School of Medicine, Shanghai, China; ^cDepartment of Imaging, Tongren Hospital, Shanghai Jiaotong University School of Medicine, Shanghai, China; ^dDepartment of General Surgery, Key Laboratory for Translational Research and Innovative Therapeutics of Gastrointestinal Oncology, Hongqiao International Institute of Medicine, Shanghai, China; ^eDepartment of Pathology, Tongren Hospital, Shanghai Jiao Tong University School of Medicine, Shanghai, China; ^fDepartment of General Surgery, Tongren Hospital, Shanghai Jiao Tong University School of Medicine, Shanghai, China; ^gDepartment of Cancer Center, Shanghai Tenth People's Hospital of Tongji University, School of Medicine, Tongji University, Shanghai, China; ^hDepartment of Urinary Surgery, Tongren Hospital, Shanghai Jiaotong University School of Medicine, Shanghai, China

ABSTRACT

Background: Pancreatic cancer (PC) is one of the most common gastrointestinal tumors globally. Former investigations discovered that circular RNAs (circRNAs) play an important role in PC development. circRNAs belong to a new class of endogenous noncoding RNAs, which have been found to mediate the progression of diverse types of tumors. Nevertheless, the roles of circRNAs and the underlying regulatory mechanisms in PC remain unknown.

Methods: In this study, our team employed next-generation sequencing (NGS) to examine the abnormal circRNA expression in PC tissues. The circRNA expression in PC cell lines and tissues was detected. Then, regulatory mechanism and targets were examined with bioinformatics analysis, luciferase reporting analysis, Transwell migration, 5-ethynyl-2'-deoxyuridine, and CCK-8 analysis. An in vivo experiment was employed to elucidate hsa_circ_0014784 roles in PC tumor growth and metastasis.

Results: The results showcased abnormal circRNA expression in PC tissues. Our lab also found that hsa_circ_0014784 expression incremented in PC tissues and cell lines, implying that hsa_circ_0014784 functioned in PC progression. hsa_circ_0014784 downregulation inhibited PC proliferation and invasion in vivo and in vitro. The bioinformatics and luciferase report data validated that both miR-214-3p and YAP1 were hsa_circ_0014784 binding partners. The overexpression of YAP1 reversed the migration, proliferation, and epithelial – mesenchymal transition (EMT) of PC cells and the angiogenic differentiation of HUVECs after miR-214-3p overexpression.

Conclusion: Taken together, our study found that hsa_circ_0014784 downregulation decremented invasion, proliferation, EMT, and angiogenesis of PC by regulating miR-214-3p/YAP1 signaling.

ARTICLE HISTORY

Received 11 October 2022
Revised 23 December 2022
Accepted 22 April 2023

KEYWORDS



Angiogenesis; epithelial–mesenchymal transition; Hsa_circ_0014784; pancreatic cancer; YAP1

Introduction

Pancreatic cancer (PC) is one of the main causes of tumor-relevant death globally and ranks fourth following colorectal, lung, and breast cancers [1]. The 5-year survival rate of PC is < 10% [2]. The neoadjuvant therapy, surgical resection, and integrative therapy targets have promoted treatment options for patients with PC. However, the lack of accurate and effective therapeutic targets for early metastasis and invasion has limited the prognosis for patients with PC [3–5]. Severely poor prognosis as well as overall survival of 10–16 months is generally

relevant to patients having unresectable or locally advanced PC [6]. The data highlights the urgency of validating the molecular regulatory network of PC to find novel or more effective therapeutic target(s).

Previous studies found that EMT and angiogenesis played an essential role in the malignant progression of tumors such as PC [7–9]. EMT is a critical biological process whereby cancer cells lose epithelial features toward a more aggressive and invasive mesenchymal phenotype. The key epithelial markers, N-cadherin and Twist, play an important role in EMT processes, which

CONTACT Dengke Yang  ydk3090@shtrhospital.com  Department of Urinary Surgery, Tongren Hospital, Shanghai Jiaotong University School of Medicine, Shanghai 200336, China

© 2023 The Author(s). Published by Informa UK Limited, trading as Taylor & Francis Group.

This is an Open Access article distributed under the terms of the Creative Commons Attribution-NonCommercial-NoDerivatives License (<http://creativecommons.org/licenses/by-nc-nd/4.0/>), which permits non-commercial re-use, distribution, and reproduction in any medium, provided the original work is properly cited, and is not altered, transformed, or built upon in any way. The terms on which this article has been published allow the posting of the Accepted Manuscript in a repository by the author(s) or with their consent.

cause damage to cell – cell adhesion and mesenchymal properties, contributing to strong cell invasiveness and metastasis of PC [10,11]. Studies also found that vascular endothelial growth factor (VEGF) induced angiogenesis, which promoted tumor growth and metastasis [12–14]. Targeted angiogenesis is a potential therapeutic agent for treating PC [15].

Increasing evidence shows that ncRNAs broadly participate in PC development [16,17]. circRNAs are ncRNAs stemming from the back-splicing of precursor mRNAs, which have stable covalent circular structures and are resistant to digestion through RNase R [18]. Compared with the linear precursors, circRNAs possess functions regardless of the host genes, such as functioning as miRNA sponges [19]. Emerging evidence has unveiled that circRNAs function as miRNA sponges to influence binding partners and are involved in different cancers [20,21]. However, the role of circRNAs in PC still needs to be discovered.

In our study, we discovered that hsa_circ_0014784 expression increased in PC tissues. The downregulation of hsa_circ_0014784 expression inhibited PC proliferation and invasion *in vitro* and *in vivo*. Finally, we proved that hsa_circ_0014784-induced yes-associated protein 1 (YAP1) promoted EMT and angiogenesis through sponging miR-214-3p in PC.

Materials and methods

Ethics statement

Our team collected PC tumor and adjacent tissues from 10 patients with PC between January 1, 2021, and September 31, 2021, in Tongren Hospital affiliated to Shanghai Jiaotong University School of Medicine, Shanghai, China. The study was supervised by the Ethics Committee in Tongren Hospital affiliated to Shanghai Jiaotong University School of Medicine. Our team informed patients and their relatives of the study, and they signed consent forms.

NGS quantification and identification of human circRNAs

RNA was obtained from freshly frozen PC tissues. Our team checked RNA quality using Agilent 2200 (Agilent Technologies, USA). Our team treated

RNA using a RiboMinus eukaryote kit (Qiagen, CA, USA) to remove ribosomal RNA, followed by cDNA library construction. NGS was conducted with Illumina HiSeq 3000 (Illumina, CA, USA). Reads were aligned to GRCH37.p13 NCBI as a reference genome. The unmapped reads were collected to characterize circRNAs, and those mapped to circRNA junction were counted for every candidate.

Cell culture and transfection

Our team cultured PC cancer cell lines SW1990, PANC-1, BxPC3, AsPC-1, Capan-2, and HPDE6-C7 cells in DMEM (Gibco, NY, USA) supplemented with 10% FBS (Gibco). The technician incubated cells at 37°C in a humidified atmosphere including 5% CO₂.

The technician transfected si-circ-0014784, YAP1 overexpression vector, and miR-214-3p inhibitor (GenePharma, Shanghai, China) into both SW1990 and PANC-1 cells utilizing Lipofectamine 2000 transfection reagent (Invitrogen) following protocols for 2 days before further analysis. RT-qPCR was used for transfection efficiency analysis.

Fluorescence *in situ* hybridization

Special probes to hsa_circ_0014784, U6, and 18S rRNA were prepared (Genesee Biotech, Guangzhou, China). Our team captured signals through Cy3-conjugated anti-biotin antibodies (Jackson ImmunoResearch Inc., PA, USA). The technician counterstained cell nuclei with 4,6-diamidino-2-phenylindole (DAPI). Finally, our team obtained images using Zeiss LSM 700 confocal microscope (Carl Zeiss, Oberkochen, Germany).

Cell counting kit assay

Our team seeded cells into 96-well plates at a density of 2×10^3 cells per well. At established time points, the absorbance at 450 nm of every sample was detected by applying CCK-8 assay (Yeasen Biotech Co., Ltd, Shanghai, China). Finally, the cell viability curve was plotted.

The 5-ethynyl-2'-deoxyuridine assay

Our lab analyzed DNA synthesis and cell proliferation by applying a 5-ethynyl-2'-deoxyuridine (EdU) assay kit (RiboBio, Guangzhou, China). Then, our team seeded 1×10^4 SW1990 and PANC-1 cells into 95-well plates overnight. On the second day, 25 μ M EdU solution was put on the plate, and the cells were incubated for 24 h. Afterward, 4% formalin was utilized to fix cells at room temperature for 2 h before 0.5% Triton X-100 to permeabilize cells for 10 min. Further, 200 μ L of Apollo reaction solution and 200 μ L of DAPI were added to stain EdU and nuclei, respectively, for 0.5 h. The technician measured DNA synthesis and cell proliferation using a Nikon microscope (Nikon, Tokyo, Japan).

Transwell migration assay

The cells transfected for 2 days were adjusted to a dose of 2.0×10^5 /mL. Briefly, 200 μ L/well cell suspension was applied to the upper side of the Transwell chamber (Millipore, MA, USA). Meanwhile, 500 μ L the medium including 10% FBS was put on the lower side. After 1 day of incubation, the invasive cells on the bottom side were fixed with methanol for 15 min and stained with crystal violet for 20 min. We observed penetrating cells under the microscope and counted invading cells. Five fields of view were selected randomly for each sample.

Quantitative real-time polymerase chain reaction

Our team obtained total RNA from cells or from the skin tissue of the wound using a TRIzol reagent kit (Invitrogen, CA, USA). The technician synthesized cDNA to amplify it using a TaqMan miRNA Reverse Transcription Kit. Our team performed quantitative polymerase chain reaction (qPCR) utilizing TaqMan MicroRNA Assay Kit (#4440885, Applied Biosystems, CA, USA). The technician employed the $2^{-\Delta\Delta CT}$ method to detect relative fold alternations in expression. *U6* and *GAPDH* were applied as internal references. The primers utilized to assay *hsa_circ_0014784* expression were forward, 5'-GACTGTAGCTTTGGAAGTTTAGCTC-3' and reverse, 5'-GUAGCACCCAGACAGCAGCAG

G-3'. *miR-214-3p* primers were forward, 5'-GCGACAGCAGGCACAGACA-3'; reverse: 5'-AGTGCAGGGTCCGAGGTATT-3'. *VEGF* primers were forward, 5'-GCCTTAGGACACCATACCGATG-3' and reverse, 5'-GCTGCCCCAGGG AACAAAGTTG-3'. *Twist-1* primers were forward, 5'-GGCACCATCCTCACACCTCT-3' and reverse, 5'-GCTGATTGGCAGCAGCCTCT-3'. *N-cadherin* primers were forward, 5'-AGCTCCATTCCGACTTAGACA-3' and reverse, 5'-CAGCCTGAGCACGAAGAGTG-3'. *U6* primers were forward, 5'-CTCGCTTCGGCAGCACA-3'; reverse: 5'-AACGCTTCACGAATTTGCGT-3'. *GAPDH* primers were forward, 5'-AATGGGCAGCCGTTAGGAAA-3'; reverse: 5'-TGAAGGGGTTCATTGTGGCA-3'.

Tube formation assay

The tube formation assay was performed as described previously [22]. In the assays, we coated 96-well plates with 50 μ L of Matrigel. We co-incubated 2×10^4 HUVECs with 200 μ L supernatants from every group for 10 min, followed by 6- to 8-h incubation at 37°C. The images were obtained with a microscope (Nikon, Tokyo, Japan). We quantified antiangiogenic activity via detecting the length of tube walls constructed between discrete endothelial cells in every well relative to controls.

Dual-luciferase reporter assay

The putative miR-214-3p-binding site in target gene *YAP1* and *hsa_circ_0014784* (Wt or Mut) 3'-UTR were cloned into psi-CHECK (Promega, WI, USA) vector downstream of firefly luciferase 3'-UTR-*YAP1* or *hsa_circ_0014784* as a primary luciferase signal with Renilla luciferase as normalization signal, which our lab named *YAP1-Wt/hsa_circ_0014784-Wt* and *YAP1-Mut/hsa_circ_0014784-Mut*. psi-CHECK vector itself supplied Renilla luciferase signal as normalization to compensate for differences between transfected and harvested efficiencies. The transfection into HEK293 cells was performed by applying Lipofectamine 2000 (Invitrogen Life Technologies). The technician captured Renilla and firefly luciferase activities 1 day post

transfection with Dual-Luciferase Reporter Assay System (Promega, Mannheim, Germany) applying a luminometer (Molecular Devices, USA). The relative Renilla luciferase activities were analyzed following protocols (Promega, Mannheim, Germany).

In vivo experiments

PANC-1 cells transfected with sh-NC or sh-circ-0014784 (2×10^6) were injected into the nude mouse flank to make nude mouse models of PC. The tumor weight and volume were measured. The Animal Ethics Committee in the Second Affiliated Hospital affiliated to Anhui Medical University supervised animal experiments.

For tumor metastasis analysis, luminescence-labeled PANC-1 cells stably transfected with sh-NC or sh-circ-0014784 were suspended in 100 μ L of phosphate-buffered saline (with 2×10^5 cells) and injected into the tail vein. The technician evaluated lung metastasis utilizing *in vivo* bioluminescence imaging system after injection for 4 weeks. The counts regarding metastatic foci in lung tissues were computed after hematoxylin-eosin (H&E) staining.

Immunohistochemical and immunofluorescence analyses

Our team fixed tissue specimens with 4% paraformaldehyde solutions and embedded them in paraffin. The technician sectioned and cultured the sections overnight with primary antibodies against CD31 or Ki67 at 4°C and with secondary antibodies (Abcam) for 1 h at 37°C. We examined and photographed sections using a Nikon microscope (Nikon).

Statistical analysis

Data were shown as means \pm standard deviation (SD). Statistical analyses were performed in GraphPad Prism (CA, USA) to determine significant differences among groups. *P* values ≤ 0.05 were regarded as statistically significant. Two-tailed Student *t* tests were used to determine

significant differences between two groups, and two-way analysis of variance with *post hoc* Bonferroni tests were used to determine significant differences among three or more groups.

Results

Hsa_circ_0014784 played a role in PC progression

A previous study found that circRNA played an important role in the progression of different cancers including PC [20]. In the present study, NGS was applied to detect circRNAs expressed differentially between PC tumor and adjacent normal tissues. The result showcased many circRNAs with abnormal expression in PC tumor tissues (Figure 1a). Our lab used RT-qPCR to further confirm the upregulation of nine circRNAs, including hsa_circ_0014784, hsa_circ_0036650, hsa_circ_0036984, hsa_circ_0037002, hsa_circ_0104953, hsa_circ_0007701, hsa_circ_0007846, hsa_circ_0037855, and hsa_circ_0037869. The data showed that hsa_circ_0014784 had the maximum upregulation level (Figure 1b). We also found that hsa_circ_0014784 expression was upregulated in 10 pairs of PC tumor tissues compared with adjacent normal tissues (Figure 1c). Fluorescence *in situ* hybridization (FISH) showcased that hsa_circ_0014784 expression incremented in PC tissues compared with adjacent normal tissues, and hsa_circ_0014784 was mainly located in the cytoplasm (Figure 1d). RT-qPCR results showed that hsa_circ_0014784 expression was upregulated in PC cell lines, including PANC-1, SW1990, AsPC-1 and BxPC3, compared with human pancreatic ductal endothelial cell line HPDE6-C7 (Figure 1e). However, only PANC-1 and SW1990 cells had higher hsa_circ_0014784 levels, and hence were selected for further study. The bioinformatics data revealed that hsa_circ_0014784 was originated from cyclizing exons from the *HDGF* gene, which was located at chr1:156711898-156713247. *HDGF* is 1349 bp, and spliced mature circRNA is 1349 (Figure 1f). Therefore, we named hsa_circ_0014784 as circ-HDGF.

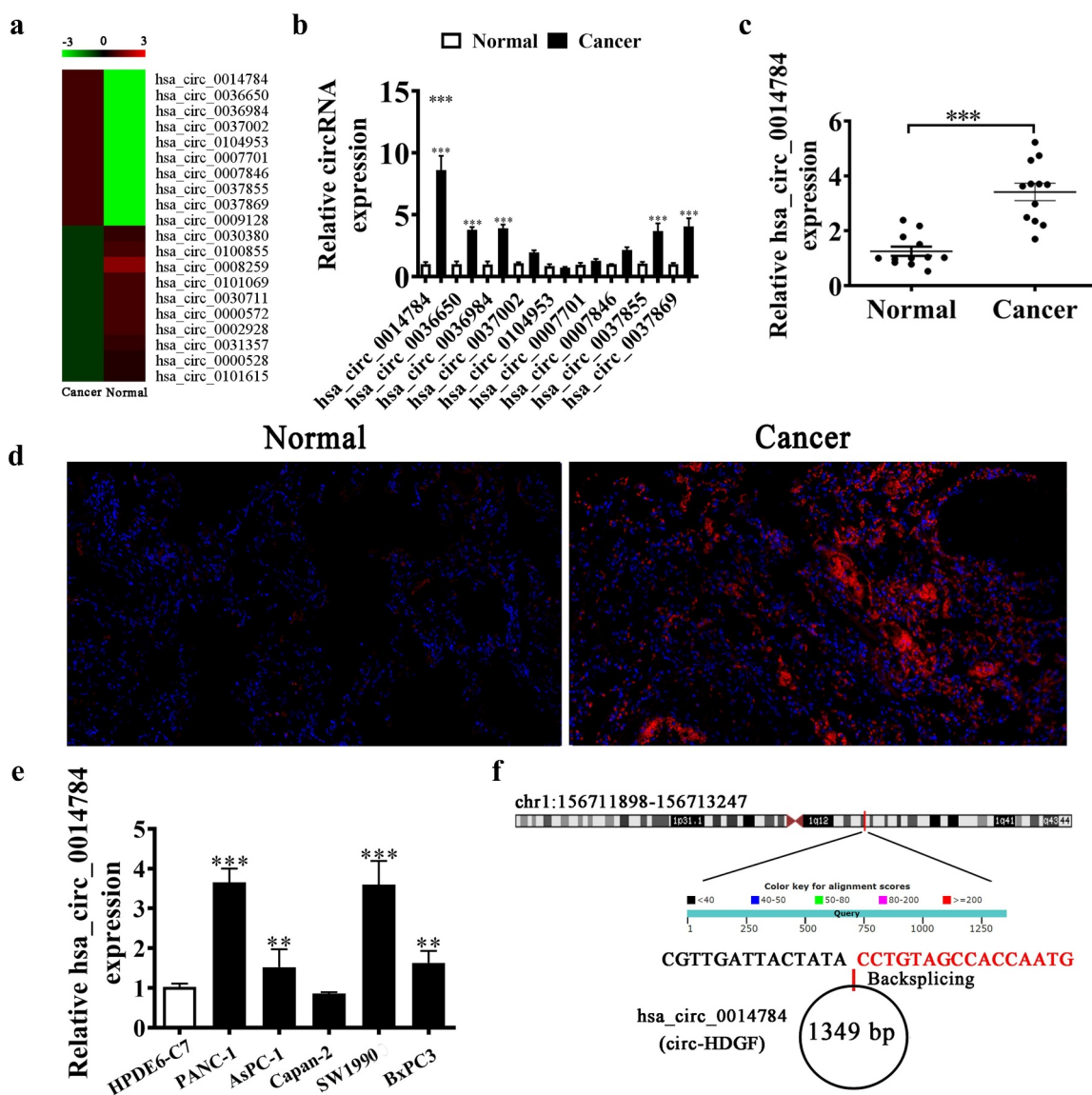


Figure 1. Hsa_circ_0014784 played a role in PC progression. (a) Heatmap showing the circRNA expression in PC tumor as well as adjacent normal tissues. (b) RT-qPCR data showed the expression of nine high-expression circRNAs in PC tumor as well as adjacent normal tissues. The results are denoted by mean \pm SD. *** P < 0.001 versus the normal tissues. (c) RT-qPCR data showed hsa_circ_0014784 expression in 10 pairs of PC tumor as well as adjacent normal tissues. The results are represented by mean \pm SD. *** P < 0.001 versus the normal tissues. (d) FISH detection showcased hsa_circ_0014784 expression and subcellular distribution. (e) RT-qPCR detection showcased hsa_circ_0014784 expression in PC cancer cell lines PANC-1, AsPC-1, Capan-2, SW1990, and BxPC3, and human pancreatic ductal endothelial cells.

(HPDE6-C7). The results are represented by mean \pm SD. ** P < 0.01, *** P < 0.001 versus HPDE6-C7. (f) Genomic loci of HDGF and hsa_circ_0014784.

Hsa_circ_0014784 downregulation inhibited PC cell growth and proliferation *in vivo* and *in vitro*

We constructed siRNA against hsa_circ_0014784 (si-circ-0014784, 5'-CUGCCUAGAUUCAGGGAAAUU-3'), which we transfected into both PANC-1 and SW1990 cells to illustrate the role of hsa_circ_0014784 in PC progression. RT-qPCR data showcased that

hsa_circ_0014784 expression significantly decremented in SW1990 and PANC-1 cells post silencing hsa_circ_0014784 (Figure 2a). CCK-8 (Figures 2b and c) and EdU (Figures 2d and e) detection found that the downregulation significantly decreased cell proliferation ability after silencing hsa_circ_0014784 in SW1990 and PANC-1 cells. The tumor formation in nude mouse xenografts using PANC-1 cells

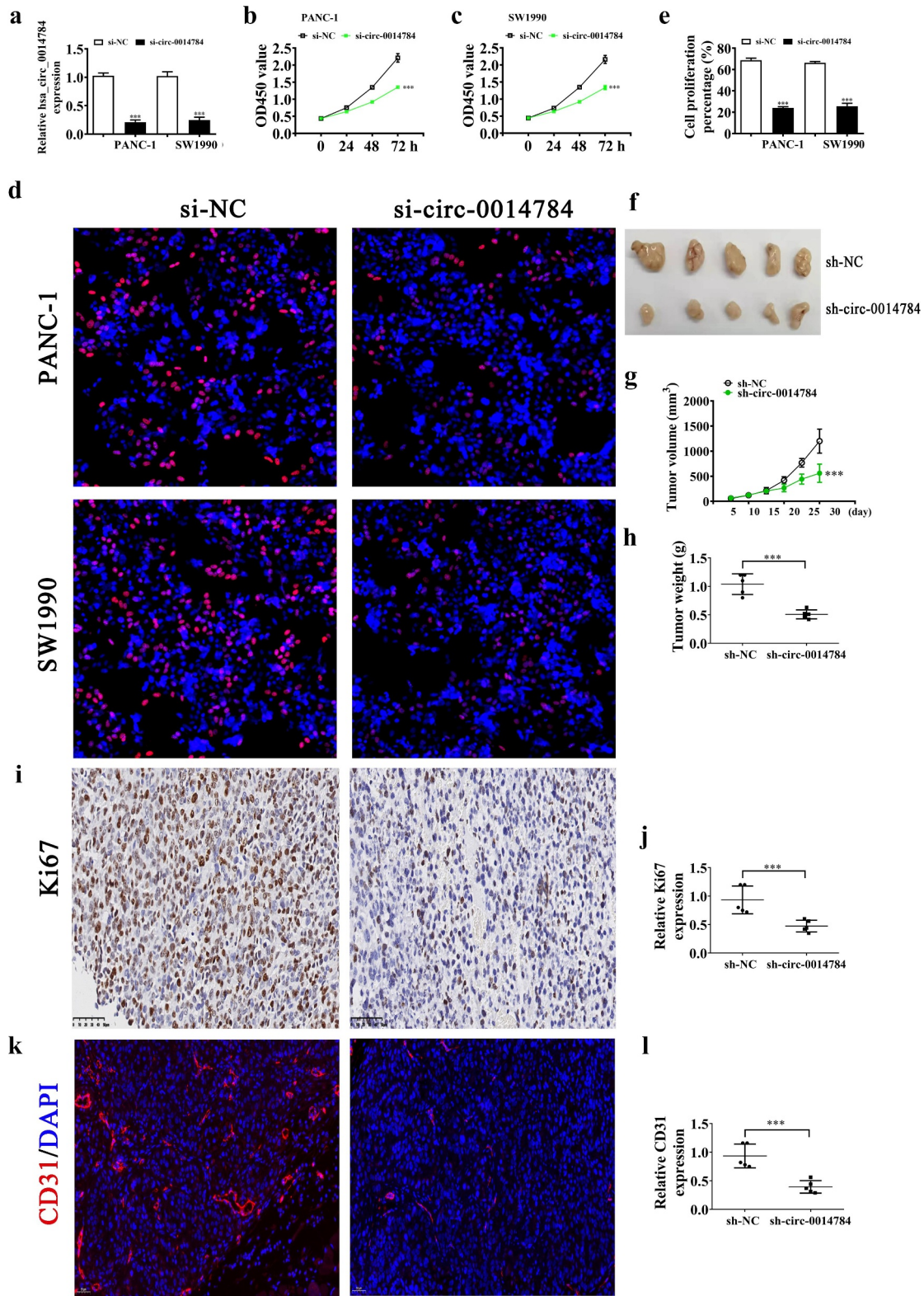


Figure 2. Hsa_circ_0014784 downregulation inhibited PC cell proliferation and tumor growth in vivo and in vitro. (a) RT-qPCR data showed hsa_circ_0014784 expression in both PANC – 1 and SW1990. The results are denoted by mean \pm SD. (b-c) CCK – 8 detection showcased hsa_circ_0014784 effects on PC cell proliferation. The data are denoted by mean \pm SD. (d-e) EdU assays showing cell proliferation in PANC – 1 and SW1990 cells. The results are represented by mean \pm SD. (f) Representative figures of PANC – 1 tumor formation in nude mouse xenografts. (g and h) Summary of tumor volumes and weight in mice. The results are expressed as mean \pm SD. (i and j) Immunohistochemical analysis showed percentages of Ki –67-positive cells. The number of relative Ki –67-positive cells was computed. The results are denoted as mean \pm SD. (k and l) Immunofluorescence detection showed CD31 expression in tumor tissues. Data are expressed as mean \pm SD. *** P < 0.001 versus sh-NC.

showcased that hsa_circ_0014784 silencing significantly decremented tumor growth in terms of weight and volume (Figure 2f–h). The immunohistochemical analysis with Ki67 staining detection also confirmed that hsa_circ_0014784 silencing inhibited Ki67 expression in tumor tissues (Figure 2i and j). The immunofluorescence for CD31 staining illustrated that hsa_circ_0014784 silencing significantly decremented tumor vascular differentiation (Figure 2k and l). This finding suggested that hsa_circ_0014784 downregulation inhibited GC proliferation, tumor growth, and tumor vascular differentiation *in vitro* and *in vivo*.

Hsa_circ_0014784 downregulation inhibited PC cell migration and pulmonary metastasis *in vivo* and *in vitro*

Transwell migration assay showcased that hsa_circ_0014784 silencing suppressed PC cell migration

(Figures 3a and b). Living imaging detection showed PANC-1 cell pulmonary metastasis and that hsa_circ_0014784 silencing reduced pulmonary metastasis ability through decremting metastatic foci numbers in lung tissues post H&E staining analyses (Figures 3c–e). It suggested that the hsa_circ_0014784 downregulation inhibited PC cell invasion.

miR-214-3p and YAP1 were hsa_circ_0014784 binding partners

Because RNA localization within cells is indispensable for their functions, our team defined the subcellular localization of hsa_circ_0014784 in PANC-1 cells. The subcellular fractionation and FISH assays advised that hsa_circ_0014784 was located mainly in the cytoplasm (Figure 4a and b). Cytoplasm-localized circRNAs mainly act as competing endogenous RNAs (ceRNAs), which are that

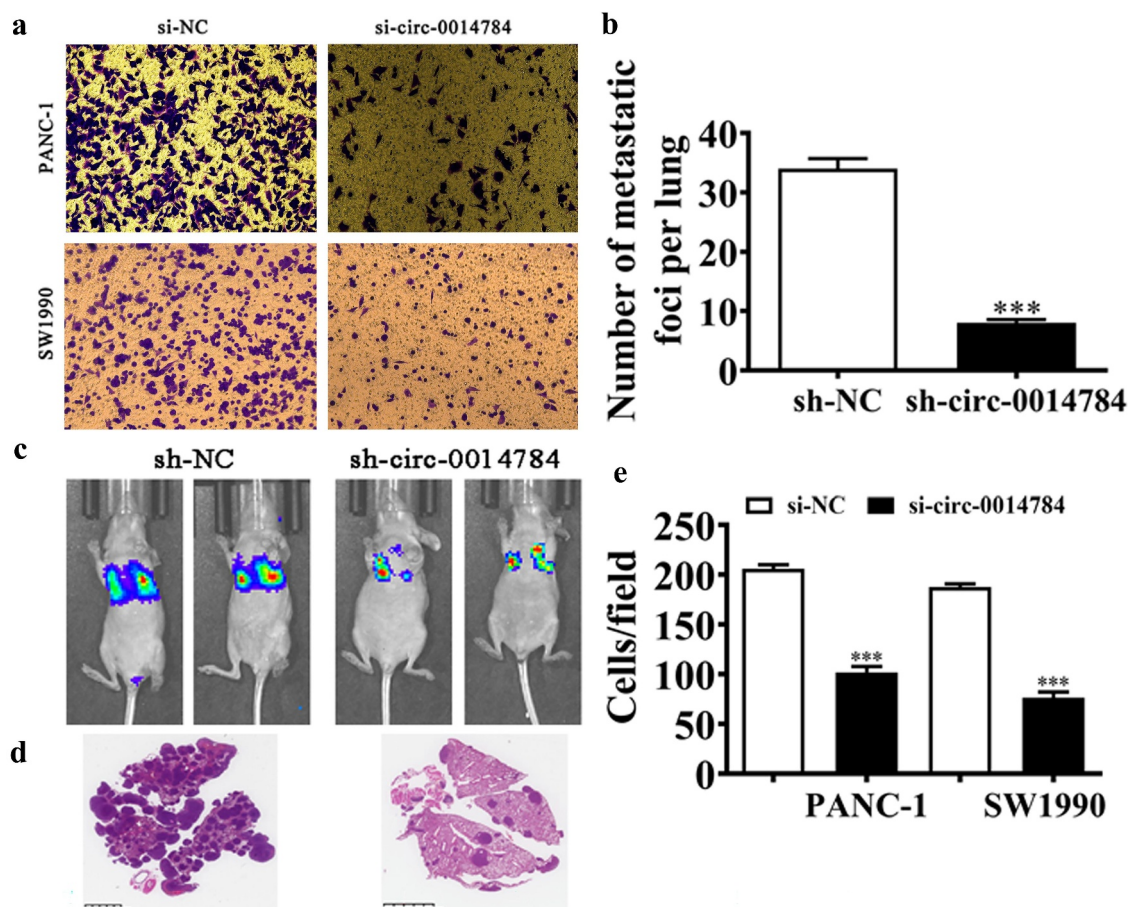


Figure 3. Hsa_circ_0014784 downregulation inhibited PC cell migration and pulmonary metastasis *in vitro* and *in vivo*. (a) Transwell detection showcased SW1990 and PANC-1 cell migration post si-circ-0014784 transfection. Results are denoted as mean \pm SD. (c) Living imaging detection showcased pulmonary metastasis in PANC-1 cells. (d–e) Counts of metastatic foci in lung tissues were computed after HE staining. Results are expressed as mean \pm SD. *** P < 0.001 versus sh-NC.

regulate each other at the post-transcription level by competing for miRNA regulators [23,24]. miRNAs bound potentially to hsa_circ_0014784 were predicted using Starbase to define whether hsa_circ_0014784 functioned as miRNA sponge in PC. Then, we constructed the luciferase reporter vector (containing the hsa_circ_0014784 sequence). Different miRNA mimics, including miR-195-5p, miR-15a-5p, miR-16-5p, miR-424-5p, miR-497-5p, miR-214-3p, miR-761, miR-873-5p, miR-212-3p, miR-200a-3p, miR-141-3p, miR-432-5p, miR-654-3p, miR-3174, and miR-4784, were transfected into HEK293. The result showcased that miR-214-3p decreased fluorescein intensity significantly. It suggested that miR-214-3p was the hsa_circ_0014784 binding partner (Figure 4c).

A luciferase reporter analysis furthermore validated that miR-214-3p suppressed luciferase activity in WT cells, but not in Mut cell lines (Figure 4d and e), suggesting that miR-214-3p was hsa_circ_0014784 target. The bioinformatics data also showed that YAP-1 was miR-214-3p binding partner. The luciferase reporter vector was constructed (Figure 4f). The luciferase reporter data showed that miR-214-3p suppressed luciferase activity in wild-type cells (Figure 4g), suggesting that YAP-1 was miR-214-3p target.

The RT-qPCR results showcased that hsa_circ_0014784 expression decremented post hsa_circ_0014784 silenced vector transfections. However, the treatment with the miR-214-3p inhibitor or overexpressing YAP-1 could not restore hsa_circ_0014784 expression in PANC-1 and SW1990 cells (Figure 4h and i). This finding suggested that both miR-214-3p and YAP-1 were hsa_circ_0014784 binding partners. The RT-qPCR results found that hsa_circ_0014784 silencing increased miR-214-3p expression. YAP-1 overexpression did not affect si-circ-0014784-induced miR-214-3p expression (Figures 4j and k). It suggested that miR-214-3p was at hsa_circ_0014784 downstream. The results showcased that hsa_circ_0014784 silencing reduced YAP-1 expression. However, the miR-214-3p downregulation reversed the inhibitory effect of si-circ-0014784 upon YAP-1 expression. After YAP-1 overexpression vector transfection, YAP-1 expressions incremented significantly (Figure 4l and m). It suggested

that hsa_circ_0014784 enhanced YAP-1 expression via sponging miR-214-3p.

YAP1 overexpression or miR-214-3p inhibition reversed the proliferation, migration, and tumor angiogenesis of PC cells after silencing hsa_circ_0014784

EdU (Figure 5a-c) detection showed that YAP1 overexpression or miR-214-3p inhibition restored cell proliferation in SW1990 and PANC-1 cells after silencing hsa_circ_0014784. Transwell migration assay also showed that YAP1 overexpression or miR-214-3p inhibition restored PC cell migration in SW1990 and PANC-1 cells postsilencing hsa_circ_0014784 (Figure 5d-f). The data also found that YAP1 overexpression or miR-214-3p inhibition restored inhibitory effect of si-circ-0014784 on the angiogenic differentiation of HUVECs (Figure 5g and h).

Overexpression of YAP1 reversed PC cell migration and proliferation along with angiogenic differentiation of HUVECs post miR-214-3p overexpression

EdU (Figure 6a-c) detection showcased that miR-214-3p overexpression suppressed PC cell proliferation in SW1990 and PANC-1 cells. However, YAP1 overexpression restored cell proliferation capabilities in PANC-1 and SW1990 cells post miR-214-3p overexpression. Transwell migration assay also showcased that YAP1 overexpression reversed PC cell migration ability post miR-214-3p overexpression in SW1990 and PANC-1 cells (Figure 6d-f). The data also showed that the YAP1 overexpression restored miR-214-3p inhibitory effects on the angiogenic differentiation of HUVECs (Figure 6g and h).

Overexpression of YAP1 or miR-214-3p inhibition reversed PANC-1 tumor growth after silencing hsa_circ_0014784

The tumor formation in xenografts of nude mice using PANC-1 cells showcased that hsa_circ_0014784 silencing significantly reduced tumor growth in terms of weight and volume, but YAP1 overexpression or miR-214-3p inhibition reversed PANC-1 tumor growth after silencing

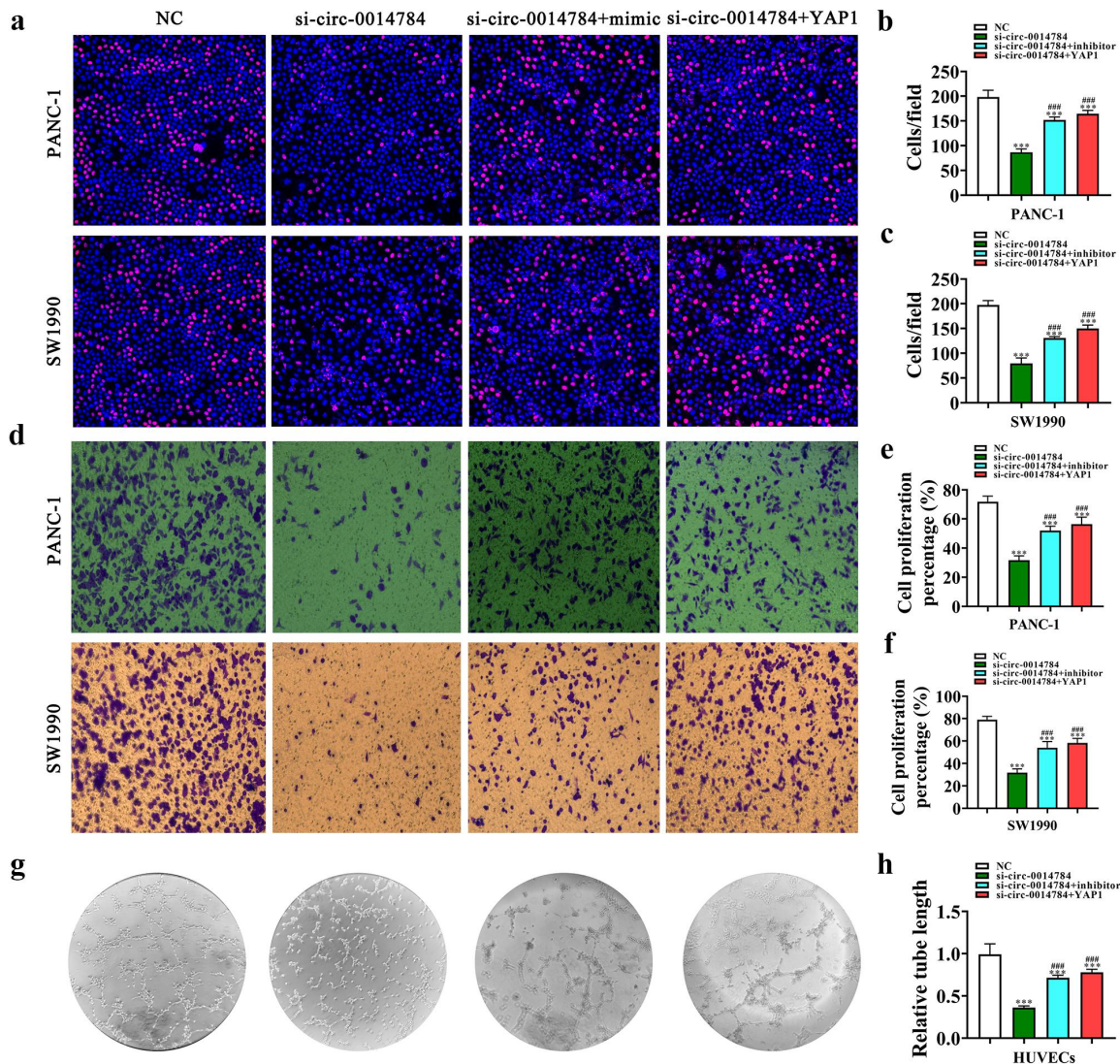


Figure 5. YAP1 overexpression or miR-214-3p inhibition reversed PC cell migration and proliferation post silencing of hsa_circ_0014784. (a – c) EdU detection showed the PANC-1 and SW1990 cell proliferation abilities. Data are represented by mean \pm SD. (d – f) Transwell detection showed the SW1990 and PANC-1 cell migration. Data are represented by mean \pm SD. (g and h) Tube formation ability of HUVECs was detected. The results are expressed as mean \pm SD. *** P < 0.001 versus NC. ### P < 0.001 versus si-circ-0014784.

hsa_circ_0014784 (Figure 7a–c). The immunohistochemical analysis with Ki67 staining detection also confirmed that YAP1 overexpression or miR-214-3p inhibition reversed the inhibitory effect of Ki67 after hsa_circ_0014784 silencing in tumor tissues (Figure 7d and 7e). The immunofluorescence for CD31 staining showcased that hsa_circ_0014784 silencing decreased tumor vascular differentiation significantly (Figure 7f and g). RT-qPCR detection showed that YAP1 overexpression or miR-214-3p inhibition restored the expression of VEGF and EMT-associated genes N-cadherin and Twist. This

finding suggested that the YAP1 overexpression or miR-214-3p inhibition reversed PANC-1 tumor growth after silencing hsa_circ_0014784.

Discussion

A previous study found that circRNA played an important role in the progression of different diseases including cancer [21]. Other investigations found that circPTPN22 attenuated immune microenvironment of PC via STAT3 acetylation [25]. Circ-EYA3 induced energy

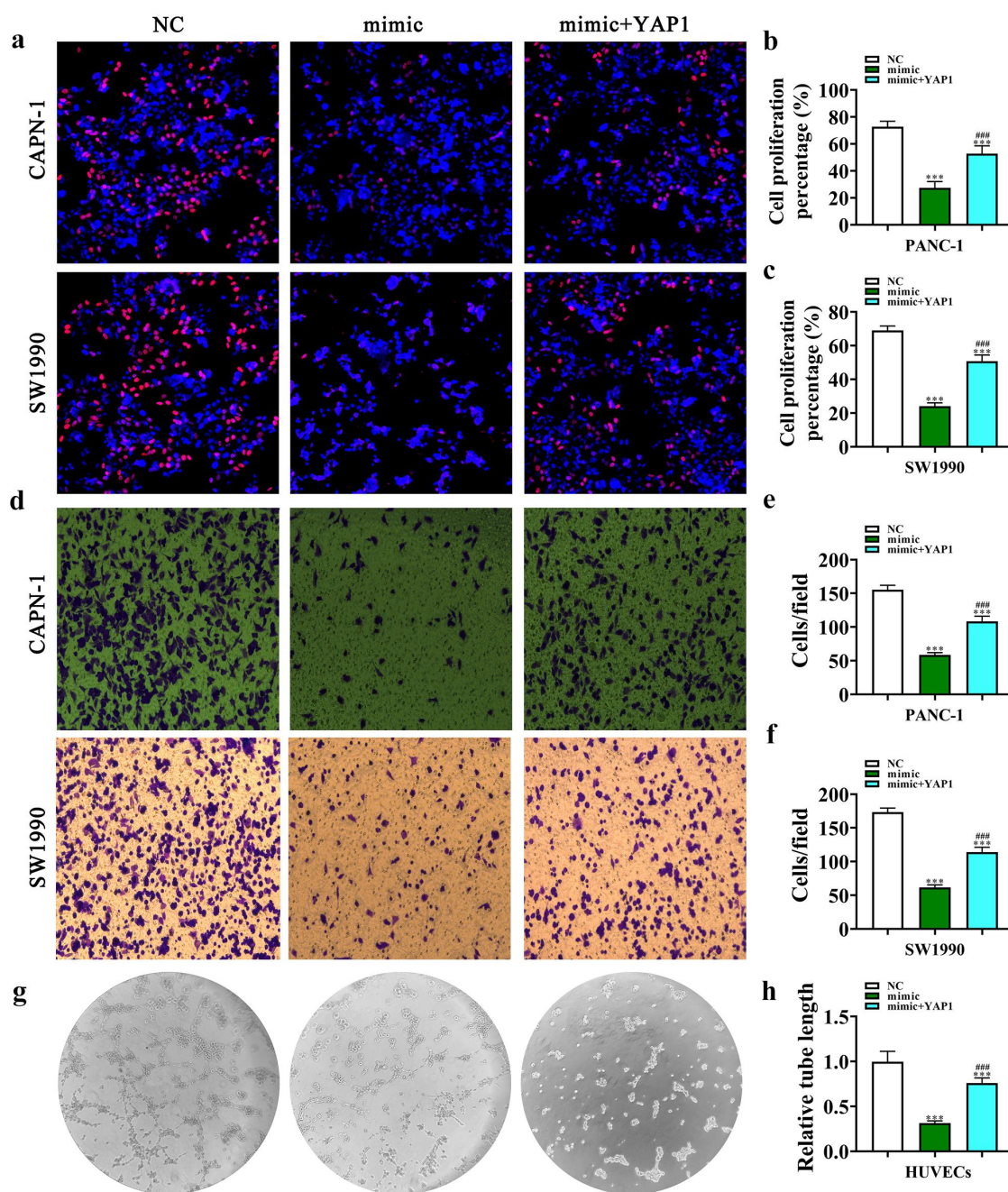


Figure 6. Overexpression of YAP1 reversed PC cell proliferation and migration along with angiogenic differentiation of HUVECs after overexpression of miR-214-3p. (a – c) EdU detection showed the proliferation capability of PANC-1 and SW1990 cells. Results are denoted as mean \pm SD. (d – f) Transwell detection illustrated PANC-1 and SW1990 cell migration. Data are represented by mean \pm SD. (g – h) Tube formation ability of HUVECs. The results are expressed as mean \pm SD. *** P < 0.001 versus NC. ### P < 0.001 versus mimic.

production to enhance the progression of pancreatic ductal adenocarcinoma through the miR-1294/c-Myc axis [26]. Nevertheless, the circRNA expression and the regulatory roles during PC have much ambiguity. In the present investigation, we discovered that hsa_circ_0014784 expression incremented in PC

tissues and cell lines. hsa_circ_0014784 was derived from the *HDGF* gene and located mainly in the cytoplasm as previously reported [27,28]. The hsa_circ_0014784 downregulation inhibited PC migration and proliferation *in vivo* and *in vitro*. It suggested that hsa_circ_0014784 played a role in the progression of PC.

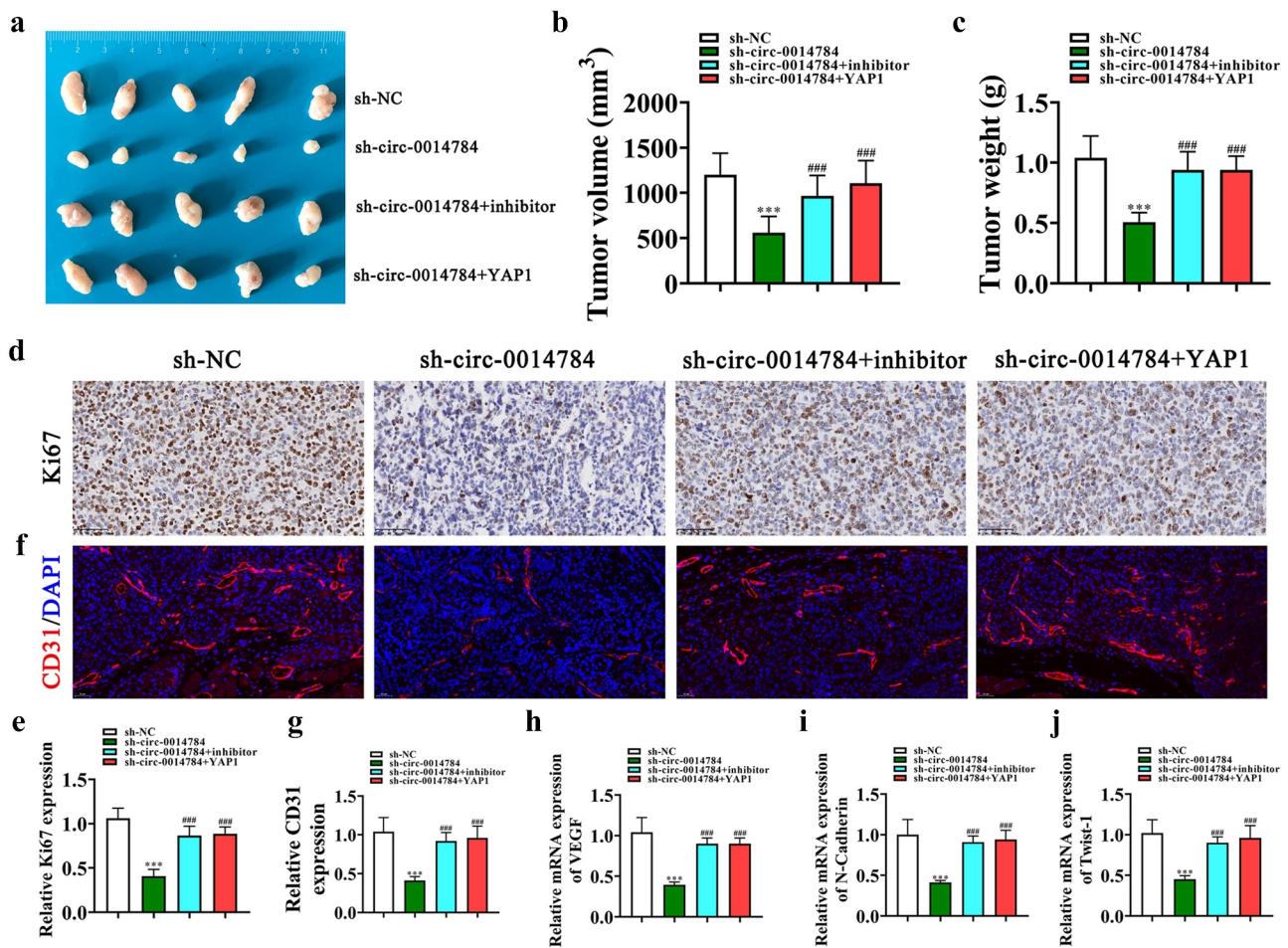


Figure 7. YAP1 overexpression or miR-214-3p inhibition reversed PANC-1 tumor growth after silencing hsa_circ_0014784. (a) Representative photographs of PANC-1 tumor formation in nude mouse xenografts. (b-c) Summary of tumor volumes and weight in mice. Results are represented by mean \pm SD. (d and e) Immunohistochemical analysis showed Ki-67-positive cell percentages. Relative numbers of Ki-67-positive cells were computed. Results are denoted as the mean \pm SD. (f-g) Immunofluorescence detection showed the CD31 expression in tumor tissues. Data are denoted as the mean \pm SD. (h-j) RT-qPCR results showed the VEGF, N-cadherin, and Twist-1 expression. Data are expressed by mean \pm SD. *** P < 0.001 versus sh-NC. ### P < 0.001 versus sh-circ-0014784.

A previous study found that circRNAs bound to miRNAs via regulatory mechanisms where endogenous RNAs competed to regulate indirectly mRNA expression corresponding to miRNA downstream target genes, contributing to PC progression [28]. Bioinformatics analysis suggested that miR-214-3p and YAP1 were hsa_circ_0014784 binding partners, which we confirmed by luciferase reporting assay. The hsa_circ_0014784 downregulation enhanced miR-214-3p expression. The altered expression of miR-214-3p is involved in tumorigenesis. It was known that miR-214-3p expression inhibited cancer proliferation and migration by regulation EMT [28-30]. The investigation discovered that miR-

-214-3p expression inhibited angiogenesis [31]. A previous study also found that miR-214-3p, as a candidate therapeutic PC target, was downregulated. miR-214-3p upregulation could inhibit PC progression [32,33]. The data showcased that miR-214-3p downregulation reversed si-circ-0014784 inhibitory effects on PC cell EMT, proliferation, migration, and angiogenesis. It suggested that hsa_circ_0014784 silencing inhibited PC progression by promoting miR-214-3p expression.

Further studies found that YAP1 was the miR-214-3p binding partner, which we verified using the luciferase reporter data. hsa_circ_0014784 downregulation suppressed YAP1 expression. However, the miR-214-3p inhibition reversed si-circ-0014784

inhibitory effects on hsa_circ_0014784 expression. YAP1 expression was upregulated in PC tissues compared with normal tissues [34–36]. The high YAP1 expression contributed to EMT and enhanced the aggressiveness of a large number of human cancers including PC [37]. Investigations also found that the high YAP1 expression promoted angiogenesis and aggressiveness of cancer [22]. In this study, our team found that YAP1 overexpression restored si_circ-0014784 inhibitory effects on PC proliferation, migration, EMT, and angiogenesis by promoting the expression of metastasis-associated molecules such as VEGFA, N-cadherin, and Twist. This finding suggested that hsa_circ_0014784 silencing inhibited PC progression via promoting miR-214-3p and inhibiting YAP1 expression.

In a word, the present investigation provided evidence that the hsa_circ_0014784 expression downregulation decremented proliferation, invasion, EMT, and angiogenesis of PC cells through miR-214-3p/YAP1 signaling regulation. All findings suggested that hsa_circ_0014784 was a candidate biomarker for PC diagnostics, which extended the drug applications targeting hsa_circ_0014784, informing the potential functions of hsa_circ_0014784 in PC treatment.

Disclosure statement

No potential conflict of interest was reported by the authors.

Funding

The author(s) reported there is no funding associated with the work featured in this article.

Authors' contributions

YB L and P W contributed to the study conception and design. All authors collected the data and performed the data analysis. All authors contributed to the interpretation of the data and the completion of figures and tables. All authors contributed to the drafting of the manuscript and final approval of the submitted version.

Availability of data and material

The datasets used and/or analyzed in this study are available from the corresponding author on reasonable request.

References

- [1] Tonini V, Zanni M. Pancreatic cancer in 2021: what you need to know to win. *World J Gastroenterol.* 2021;27(35):5851–5889. DOI:10.3748/wjg.v27.i35.5851.
- [2] Park W, Chawla A, O'Reilly EM. Pancreatic Cancer: a Review. *JAMA.* 2021;326(9):851–862. DOI:10.1001/jama.2021.13027.
- [3] Strobel O, Neoptolemos J, Jäger D, et al. Optimizing the outcomes of pancreatic cancer surgery. *Nat Rev Clin Oncol.* 2019;16(1):11–26. DOI:10.1038/s41571-018-0112-1
- [4] Versteijne E, Vogel JA, Besselink MG, et al. Meta-analysis comparing upfront surgery with neoadjuvant treatment in patients with resectable or borderline resectable pancreatic cancer. *Br J Surg.* 2018;105(8):946–958. DOI:10.1002/bjs.10870
- [5] Reingold M, O'Reilly EM, Varghese AM, et al. Association of ablative radiation therapy with survival among patients with inoperable pancreatic cancer. *JAMA Oncol.* 2021;7(5):735–738. DOI:10.1001/jamaoncol.2021.0057
- [6] Buss EJ, Kachnic LA, Horowitz DP. Radiotherapy for locally advanced pancreatic ductal adenocarcinoma. *Semin Oncol.* 2021;48(1):106–110. DOI:10.1053/j.seminoncol.2021.02.005.
- [7] Fang X, Cai Y, Xu Y, et al. Exosome-mediated lncRNA SNHG11 regulates angiogenesis in pancreatic carcinoma through miR-324-3p/VEGFA axis. *Cell Biol Int.* 2022;46(1):106–117. DOI:10.1002/cbin.11703.
- [8] Guo Y, Xiao Y, Guo H, et al. The anti-dysenteric drug fraxetin enhances anti-tumor efficacy of gemcitabine and suppresses pancreatic cancer development by antagonizing STAT3 activation. *Aging.* 2021;13(14):18545–18563. DOI:10.18632/aging.203301
- [9] Ala M. Target c-Myc to treat pancreatic cancer. *Cancer Biol Ther.* 2022;23(1):34–50. DOI:10.1080/15384047.2021.2017223.
- [10] Gaianigo N, Melisi D, Carbone C. EMT and Treatment Resistance in Pancreatic Cancer. *Cancers (Basel).* 2017;9(9):122. DOI:10.3390/cancers9090122.
- [11] Huang L, Chen S, Fan H, et al. GINS2 promotes EMT in pancreatic cancer via specifically stimulating ERK/MAPK signaling. *Cancer Gene Ther.* 2021;28(7–8):839–849. DOI:10.1038/s41417-020-0206-7
- [12] Zhu HY, Gao YJ, Wang Y, et al. LncRNA CRNDE promotes the progression and angiogenesis of pancreatic cancer via miR-451a/CDKN2D axis. *Transl Oncol.* 2021;14(7):101088. DOI:10.1016/j.tranon.2021.101088
- [13] Belvedere R, Morretta E, Novizio N, et al. The Pyrazolyl-Urea Gege3 Inhibits the Activity of ANXA1 in the angiogenesis induced by the pancreatic cancer derived EVs. *Biomolecules.* 2021;11(12):1758. DOI:10.3390/biom11121758
- [14] Maharjan CK, Umesalma S, Kaemmer CA, et al. RABL6A promotes pancreatic neuroendocrine tumor angiogenesis and progression in vivo. *Biomedicines.* 2021;9(6):633. DOI:10.3390/biomedicines9060633

- [15] Ueda G, Matsuo Y, Murase H, et al. 10Z-Hymenialdisine inhibits angiogenesis by suppressing NF- κ B activation in pancreatic cancer cell lines. *Oncol Rep.* 2022;47(3). DOI:10.3892/or.2022.8259
- [16] Ju X, Tang Y, Qu R, et al. The emerging role of Circ-SHPRH in Cancer. *Onco Targets Ther.* 2021;14:4177–4188. DOI:10.2147/OTT.S317403
- [17] Xu P, Xu X, Zhang L, et al. Hsa_circ_0060975 is highly expressed and predicts a poor prognosis in gastric cancer. *Oncol Lett.* 2021;22(2):619. DOI:10.3892/ol.2021.12880
- [18] Wang Y, Li Z, Xu S, et al. Novel potential tumor biomarkers: circular RNAs and exosomal circular RNAs in gastrointestinal malignancies. *J Clin Lab Anal.* 2020;34(7):e23359. DOI:10.1002/jcla.23359
- [19] Panda AC. Circular RNAs Act as miRNA Sponges. *Adv Exp Med Biol.* 2018;1087:67–79.
- [20] Rong Z, Xu J, Shi S, et al. Circular RNA in pancreatic cancer: a novel avenue for the roles of diagnosis and treatment. *Theranostics.* 2021;11(6):2755–2769. DOI:10.7150/thno.56174
- [21] Chen S, Chen C, Hu Y, et al. The diverse roles of circular RNAs in pancreatic cancer. *Pharmacol Ther.* 2021;226:107869. DOI:10.1016/j.pharmthera.2021.107869
- [22] Sun Z, Ou C, Liu J, et al. YAP1-induced MALAT1 promotes epithelial-mesenchymal transition and angiogenesis by sponging miR-126-5p in colorectal cancer. *Oncogene.* 2019;38(14):2627–2644. DOI:10.1038/s41388-018-0628-y
- [23] Kristensen LS, Andersen MS, Stagsted LVW, et al. The biogenesis, biology and characterization of circular RNAs. *Nat Rev Genet.* 2019;20(11):675–691. DOI:10.1038/s41576-019-0158-7
- [24] Zhang HD, Jiang LH, Sun DW, et al. CircRNA: a novel type of biomarker for cancer. *Breast Cancer.* 2018;25(1):1–7. DOI:10.1007/s12282-017-0793-9
- [25] He Y, Han P, Chen C, et al. circPTPN22 attenuates immune microenvironment of pancreatic cancer via STAT3 acetylation. *Cancer Gene Ther.* 2021;30(4):559–566. DOI:10.1038/s41417-021-00382-w
- [26] Rong Z, Shi S, Tan Z, et al. Circular RNA CircEYA3 induces energy production to promote pancreatic ductal adenocarcinoma progression through the miR-1294/c-Myc axis. *Mol Cancer.* 2021;20(1):106. DOI:10.1186/s12943-021-01400-z
- [27] Guo X, Zhou Q, Su D, et al. Circular RNA circBFAR promotes the progression of pancreatic ductal adenocarcinoma via the miR-34b-5p/MET/Akt axis. *Mol Cancer.* 2020;19(1):83. DOI:10.1186/s12943-020-01196-4
- [28] Liu X, Zhou L, Chen Y, et al. CircRNF13 promotes the malignant progression of pancreatic cancer through targeting miR-139-5p/IGF1R Axis. *J Oncol.* 2021;2021:1–15. doi: 10.1155/2021/6945046
- [29] Tao W, Cao C, Ren G, et al. Circular RNA circCPA4 promotes tumorigenesis by regulating miR-214-3p/TGIF2 in lung cancer. *Thorac Cancer.* 2021;12(24):3356–3369. DOI:10.1111/1759-7714.14210
- [30] Han LC, Wang H, Niu FL, et al. Effect miR-214-3p on proliferation and apoptosis of breast cancer cells by targeting survivin protein. *Eur Rev Med Pharmacol Sci.* 2019;23(17):7469–7474. DOI:10.26355/eurrev_201909_18856
- [31] Wang X, Li X, Li J, et al. Mechanical loading stimulates bone angiogenesis through enhancing type H vessel formation and downregulating exosomal miR-214-3p from bone marrow-derived mesenchymal stem cells. *FASEB J.* 2021;35(1):e21150. DOI:10.1096/fj.202001080RR
- [32] Ren H, Wei ZC, Sun YX, et al. ATF2-induced overexpression of lncRNA LINC00882, as a novel therapeutic target, accelerates hepatocellular carcinoma progression via sponging miR-214-3p to upregulate CENPM. *Front Oncol.* 2021;11:714264. DOI:10.3389/fonc.2021.714264
- [33] Kuninty PR, Bojmar L, Tjomsland V, et al. MicroRNA-199a and -214 as potential therapeutic targets in pancreatic stellate cells in pancreatic tumor. *Oncotarget.* 2016;7(13):16396–16408. DOI:10.18632/oncotarget.7651
- [34] Liu M, Zhang Y, Yang J, et al. Zinc-dependent regulation of ZEB1 and YAP1 coactivation promotes epithelial-mesenchymal transition plasticity and metastasis in pancreatic cancer. *Gastroenterology.* 2021;160(5):1771–83.e1. DOI:10.1053/j.gastro.2020.12.077
- [35] Kapoor A, Yao W, Ying H, et al. Yap1 activation enables bypass of oncogenic Kras addiction in pancreatic cancer. *Cell.* 2014;158(1):185–197. DOI:10.1016/j.cell.2014.06.003
- [36] Kapoor A, Yao W, Ying H, et al. Yap1 activation enables bypass of oncogenic kras addiction in pancreatic cancer. *Cell.* 2019;179(5):1239. DOI:10.1016/j.cell.2019.10.037
- [37] Ben Q, An W, Sun Y, et al. A nicotine-induced positive feedback loop between HIF1A and YAP1 contributes to epithelial-to-mesenchymal transition in pancreatic ductal adenocarcinoma. *J Exp Clin Cancer Res.* 2020;39(1):181. DOI:10.1186/s13046-020-01689-6